Simulation and experimental studies on the behaviour of a magnetorheological damper under impact loading

Alif Zulfakar bin Pokaad*

Department of Engineering and Technology,
University Multimedia (MMU),
Jalan Ayer Keroh Lama, Bukit Beruang, 75450 Melaka, Malaysia
E-mail: alif_zul85@yahoo.com
*Corresponding author

Khisbullah Hudha and
Mohd Zakaria bin Mohamad Nasir

Faculty of Mechanical Engineering,
Universiti Teknikal Malaysia Melaka (UTeM),
Ayer Keroh, 75450 Melaka, Malaysia
E-mail: khisbullah@utem.edu.my
E-mail: mzakaria@utem.edu.my

Ubaidillah

Department of Mechatronics,
Electronic Engineering Polytechnic Institute of Surabaya (EEPIS),
Kampus ITS Sukolilo, Surabaya 60111, Indonesia
E-mail: ubaid.ubaidillah@gmail.com

Abstract: This paper is aimed to model behaviour of a magnetorheological (MR) damper under impact loading through polynomial approach. The polynomial model is developed based on curve fitting from experimental results and consists of a three regions namely fluid locking, positive and negative acceleration regions. The experimental results which have been performed using impact test apparatus are evaluated in the form of transmitted force in velocity, displacement, and time domain. The simulation results of the proposed polynomial model are then compared with the experimental results. Results show that the proposed polynomial model closely follow the experimental data in the three regions under study namely fluid locking, positive and negative accelerations.

Keywords: magnetorheological damper; polynomial model; non-parametric technique; fluid locking; impact loading.

Reference to this paper should be made as follows: Pokaad, A.Z.b., Hudha, K., Nasir, M.Z.b.M. and Ubaidillah (2011) 'Simulation and experimental studies on the behaviour of a magnetorheological damper under impact loading', *Int. J. Structural Engineering*, Vol. 2, No. 2, pp.164–187.

Biographical notes: Alif Zulfakar bin Pokaad received his BEng of Mechanical Engineering (Automotive) from the Universiti Teknikal Malaysia Melaka (UTeM). Currently, he is a Research Assistant and MA student in Autotronic Laboratory, Faculty of Mechanical Engineering, Universiti Teknikal Malaysia Melaka (UTeM). His research project lies on magnetorheological fluid devices such as MR damper for vehicle application. He is currently a Teaching Staff at the University Multimedia Malacca.

Khisbullah Hudha received his BEng of Mechanical Design from Bandung Institute of Technology (ITB) Indonesia; MSc in the Department of Engineering Production Design, Technische Hoogeschool Utrecht, the Netherlands; and his PhD on Intelligent Vehicle Dynamics Control Using Magnetorheological Damper from Malaysia University of Technology (UTM). His research interests include modelling, identification and force tracking control of semi-active damper, evaluation of vehicle ride and handling, electronic chassis control system design and intelligent control. He is currently attached with Universiti Teknikal Malaysia Melaka (UTeM). His profile can be reached at http://www.utem.edu.my/fkm/smac/index.htm.

Mohd Zakaria bin Mohamad Nasir received his BEng in Mechanical Engineering (Automotive) form the Universiti Teknologi Malaysia (UTM) and MSc in Automotive Engineering from Coventry University, UK. His research interests are in vehicle dynamics and control fields. Currently, he is serving as Lecturer in Automotive Department, Universiti Teknikal Malaysia Melaka (UTeM).

Ubaidillah received his BEng of Mechanical Engineering from the Institut Teknologi Sepuluh Nopember (ITS) Surabaya, Indonesia. Currently, he is a Research Assistant and MA student in Autotronic Laboratory, Faculty of Mechanical Engineering, Universiti Teknikal Malaysia Melaka (UTeM). His research project lies on magnetorheological fluid devices such as MR damper, MR brake and MR engine mounting for vehicle application. He is currently a Teaching Staff at the Electronic Engineering Polytechnic Institute of Surabaya (EEPIS/PENS).

1 Introduction

Magnetorheological (MR) fluids fall into a class of smart fluids which rheological properties (elasticity, plasticity, or viscosity) change in the presence of a magnetic field. MR fluids consist of a carrier fluid, typically, a synthetic or silicone based oil, and ferromagnetic particles (20–50 μm in diameter) (Ahmadian et al., 2002). In the presence of a magnetic field, the particles align and form linear chains parallel to the field direction. With a properly designed magnetic circuit, the apparent yield stress of the MR fluid will change within milliseconds (Phule, 2001). When electromagnets are used to generate the magnetic fields, the apparent yield stress is controlled by the supply current. Increasing the supply current, the magnetic field leads to an increase in the apparent yield stress. A significant amount of work on developing electromagnetic circuits for damper coil has lead to design an electromagnetic systems that require low voltages and exhibit fast response times (El Wahed et al., 2002; Yang et al.,2002).

An MR damper is relatively a recent damping device, in which the magnitude of the resisting force acting upon a mechanical structure can be adjusted in real time (Roschke and Atray, 2002). To evaluate the potential benefits of MR dampers in vibration control applications and to take the full advantage of these devices, it is necessary to develop a model that can accurately describe the behaviour of the MR damper. Generally, there are two ways in modelling of MR damper namely parametric and non-parametric modelling (Song, 1999; Giuclea et al., 2004; Ang et al., 2004). In parametric modelling, the behaviour of MR damper is represented by a set of mathematical equations that relates the state variables and the resisting force produced by MR damper (Butz and Styrk, 1999). On the other hand, non-parametric models of MR damper known as black box model are developed by using approximation functions to estimate the trend of experimental data in the form of force versus velocity or force versus displacement characteristics (Ahmadian and Song, 1999).

There are two common approaches in non-parametric modelling. The first approach uses mathematical function such as hyperbolic tangent (Ahmadian and Song, 1999), Chebishev polynomial fit (Ehrgott and Masri, 1992), polynomial approach (Choi et al., 2001), arc-tangent model (Ang et al., 2004), sigmoid function (Wang et al., 2005) and linearised data driven model based on applied voltage and damper velocity resulting a damper force (Hudha, 2005). The second approach uses intelligent paradigm such as neural networks (Chang and Roschke, 1999), fuzzy logic (Schurter and Roschke, 2000; Peschel and Roschke, 2001) and genetic algorithm (Sireteanu et al., 2001; Giuclea et al., 2004). The non-parametric techniques are preferable since the modelling results are better in capturing the actual behaviour of a MR damper. This is due to the importance of developing a good mechanical model which is required in applying control strategy for both actuator and plant controls.

Previous studies on shock reduction are actively accomplished using smart fluid which has reversible properties with applied magnetic fields. Lee et al. (2002) investigated a MR damper to reduce shock transmitted to a helicopter including its dynamics model and controller strategy. MR damper application for shock reduction in weapon mechanism has also studied by Ahmadian et al. (2002). Song et al. (2004) proposed the shock damper to reduce impact by means of acceleration decrement of the damper. Other application was the use of MR damper in driver seat for shock attenuation. Investigation on the potential benefits of MR damper in reducing the incidence and severity of end-stop impacts of a low natural frequency was performed by McManus et al. (2002). Sapinski and Rosol (2007) also investigated the performance of MR damper applied in driver seat using open-loop and close-loop controllers. However, the previously mentioned studies did not investigate specifically in modelling the MR damper characteristics under impact loading.

The properties of MR damper have much difference between impact and harmonic loads in which the elastic and damping coefficients of MR damper enlarge greatly under impact loads (Hengbao et al., 2008). The modelling of MR damper under impact loading is important especially to predict the isolation performance in shock conditions. At presents, the mechanical models of MR damper are all derived from experiment subjected to harmonic loads. Only few studies investigate the modelling of the MR damper under impact loading. Some previous works that relate with MR damper modelling under impact load are as follows. Ahmadian and Norris (2007) investigated experimentally the behaviour of MR damper under impact loads, resulting in a MR damper model based on accumulator behaviour. Woo et al. (2007) proposed an

active bumper employing MR damper, in which the study resulted a MR damper model derived based on fluid flow dynamics. Hengbao et al. (2008) have also conducted an experimental study on MR damper behaviour under impact load and the model were derived based on modified Boucwen. Two parameters within modified Boucwen namely elastic and damping coefficient were defined based on least square fitting. However, the comparison results of Hengbao's work were only in the form of force versus time.

All these previous studies use parametric technique in deriving the MR damper model. The contribution of this work is to study behaviour of the MR damper under impact condition and develop its mathematical model which can be integrated with a control system by using non-parametric method. In order to achieve the aim, a type of MR damper is tested using impact test apparatus developed in Autotronics Laboratory, UTeM. Thus, its behaviour is investigated in both experimental and simulation studies. The experimental results are evaluated in terms of the transmitted force versus damper velocity and the transmitted force versus damper displacement. A polynomial approach is used to model the MR damper behaviour under impact loading based on its experimental results and then simulated using well-known mathematics software namely SIMULINK-MATLAB. The simulation results are then validated with variations of pendulum mass and input currents.

This paper is organised as follows: Section 1 discusses some previous works on the use of the MR damper and some techniques on MR damper modelling; Section 2 describes the experimental works for obtaining the data of MR damper test under impact loads; Section 3 explains the algorithm of the proposed modelling approach; Section 4 shows the simulation results, validation of the model with experimental data, and the last section consists of some discussion and recommendation for future study.

2 MR damper configuration and experimental setup

An MR damper is filled with a controllable fluid that contains dispersed micron-sized magnetically polarisable particles. When the fluid is subjected to magnetic field, the particles are arranged in a pattern and the behaviour of the fluid is changed from being linear viscous to semi-solid in milliseconds. By adjusting the current within an allowable range, the resisting force to motion of the MR damper increases or decreases in a non-linear fashion. When various magnitudes and patterns of current are applied to the MR damper, resistance of the damper to motion can be adjusted. A schematic of a typical MR damper is illustrated in Figure 1.

The experimental investigation of force versus velocity and force versus displacement characteristics of the MR damper needs to be performed the data for identification of the proposed the MR damper. Based on the experimental data, a modelling method of the MR damper was realised numerically using a polynomial equation.

The MR damper used in this study is RD-8040-1, which was manufactured by Lord Corporation. The damper consists of a piston, magnetic circuit, accumulator, and pressurised gas inside an accumulator and MR fluid. The length of the damper is 21 cm in its extended position and has 5 cm of stroke. The maximum current can be applied to the electromagnet coils in the magnetic choke is 2 amp and the coil r esistance is 2 ohm.

Figure 1 Schematic of an MR damper

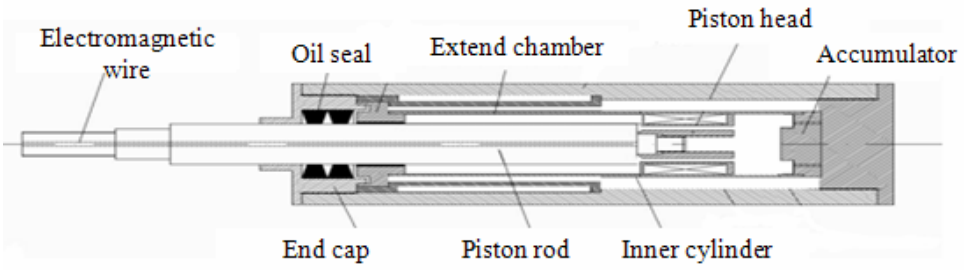

The experimental work was carried out in the Autotronic Laboratory, Department of Automotive, Universiti Teknikal Malaysia Melaka (UTeM) using a impact test rig developed by the Smart Material and Automotive Control Group, UTeM. The impact test rig consists of a wire transducer to measure the relative displacement and relative velocity of the damper and load cell to measure the damper force. The integrated measurement and control (IMC) device provides signal processing of the transducers and excitation signals of the slider crank actuator system. These signals are digitally processed and stored in a personal computer using FAMOS control software. IMC device is connected to the personal computer using NetBEUI protocol. Control signals to the MR damper are converted to analogue signals by the IMC device. Then, the voltage signals are passed through the current driver and sent to the MR damper. The setup of the impact test rig is shown in Figure 2, which is mainly composed of pendulum as the external force, MR damper and vehicle model as the basement that is fixing to the floor to make it unmovable.

Figure 2 Impact loading test rig that available at Autotronic Laboratory (see online version for colours)

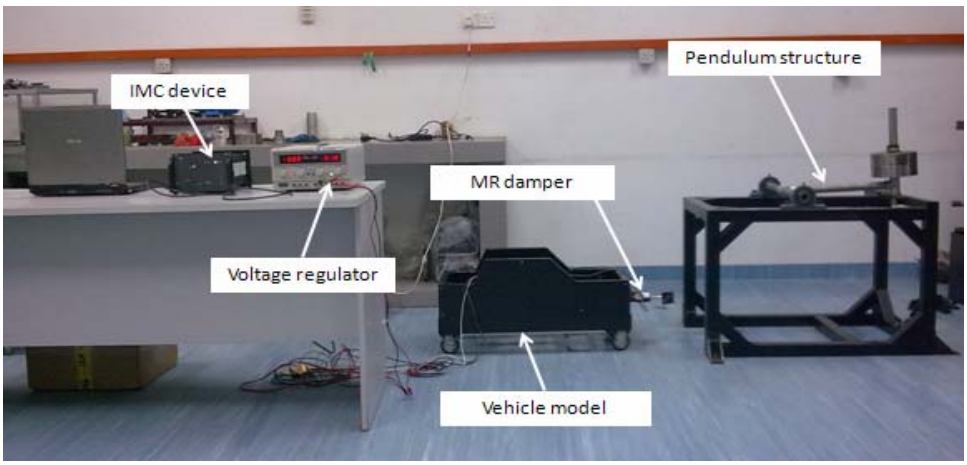

The MR damper testing was done by applying an impact loading that generated by the pendulum mass as the external force to the MR damper for different values of applied currents to the damper coils. The response of the MR damper due to impact loading 25 kg

of pendulum mass was investigated for five constant currents of 0, 0.5, 1, 1.5 and 2 ampere, being applied by the current driver of the MR damper.

3 MR damper modelling

In this work, a proposed polynomial model is investigated to predict the field-dependent damping force characteristic of the damper. The model is in a class of non-parametric techniques which employs analytical formulation to describe the characteristics of the device based on testing data analysis and the MR damper working principle. In order to build an easy implementation of MR damper model for both simulation and real time control systems, the proposed model should be develop based on the experimental data. Figure 3 shows a hard point in damper velocity and transmitted force versus time during impact load.

Figure 3 Hard point for (a) damper velocity versus time and (b) force transmitted versus time (unloading and impact loading boundary)

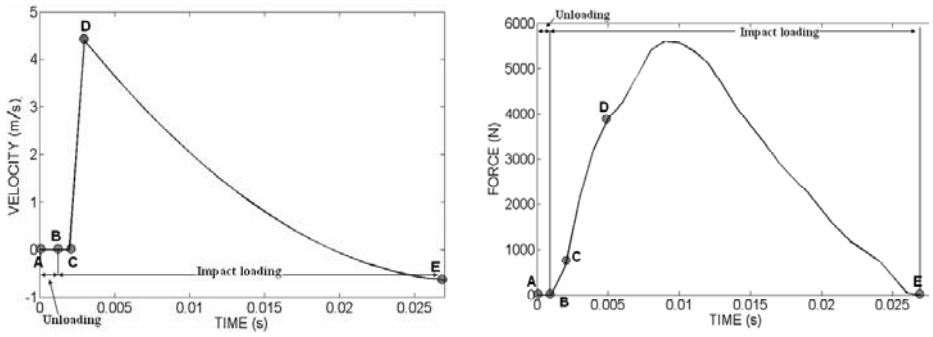

(a) (b)

Unloading boundary is defined as a term that is used to describe the pendulum in not in collision with the MR damper. The time for the unloading boundary is 0 to 0.001 s. After 0.001 s, the pendulum starts to collide with the MR damper. The impact loading boundary is defined as the time contact (t_c) between pendulum and MR damper during collision or impact. In this boundary, it is introduced three terms namely a fluid locking region, positive acceleration and negative acceleration region of MR damper during as shown in Table 1.

Table 1 Impact loading region

	Impact loading region		
	Fluid locking	*Positive acceleration*	*Negative acceleration*
Hard point	B to C	C to D	D to E
Time (s)	$0.001 < t < 0.002$	$0.002 < t < 0.005$	$0.005 < t < t_c$

During the initial stages of the impact, the transmitted force starts a rise from point B to point C. But the velocity of the damper is still zero from point B to point C, which means the damper does not move or retract. This is due to the MR fluid that does not flow through the gap at a rate that would allow the piston to enter the housing (Ahmadian and

Norris, 2008). This type of behaviour will be termed as a fluid locking region. In the most extreme case of fluid locking, the MR fluid would be trapped and the MR damper response would be solely due to the compression of the MR fluid. After 0.002 s, the MR damper starts to retract and achieve a maximum velocity at the time of 0.005 s as shown at point D. This happen is caused by the external force had overcome the fluid inertia that preventing the fluid from accelerating fast and the effect is the fluid flow fastening in the gap. This situation is called positive acceleration region for MR damper. The negative acceleration region happens because of the accumulator give the reaction to reduce the velocity of the damper. The accumulator is pushing the damper into opposite direction of the external force (pendulum). The effect is the highest transmitted force is occurred in the negative acceleration region of MR damper. The equation of the transmitted force by the MR damper under impact loading is shown below:

$$F(t) = \alpha_m f_d(I, t) \tag{1}$$

where

$F(t)$ transmitted force by MR damper

α_m dimension less parameter for transmitted force at each mass of pendulum

f_d damping force at mass of pendulum 25 kg

I current input.

In this equation, the damping force depends on the current input for MR damper and time when the impact loading is occurred. The equation for velocity of the damper during impact is described as follows:

$$v(t) = \beta_m v_d(I, t) \tag{2}$$

where

$v(t)$ velocity of the damper

β_m dimension less parameter for velocity of the damper

v_d velocity of the damper at mass of pendulum 25 kg

I current input

t time during impact loading.

The function of the dimension less parameter, α_m is to measure the force transmitted at the different pendulum mass and it is the ratio of the peak force with the pendulum mass, 15 and 20 kg divided with the peak force transmitted at mass 25 kg. The dimension less parameter will reduce the transmitted force if the pendulum mass is less than 25 kg. This is because the equation of damping force, f_d is based on the result of transmitted force at pendulum mass equal to 25 kg. The equation of the dimension less parameter for force transmitted is shown below:

$$\alpha_m = \frac{F_{speak\ (mass\ of\ 15,\ 20\ and\ 25\ kg)}}{F_{speak\ (mass\ of\ 25\ kg)}} \tag{3}$$

where

F_{peak} maximum transmitted force at each of pendulum mass.

In case to find the transmitted force of the MR damper in the variations mass of the pendulum, the curve fitting is utilised in Figure 4 between dimension less parameter, α_m and the mass of pendulum for each data in Table 2. If the pendulum mass is 25 kg, the dimension less, α_m is equal to one. The equation of the dimension less parameter after curve fitting is:

$$\alpha_m = -0.00129\left(m_p\right)^2 + 0.072404 m_p \tag{4}$$

where

m_p pendulum mass.

Figure 4 Curve fitting of the dimension less parameter, α_m and β_m for force transmitted and velocity of the damper (see online version for colours)

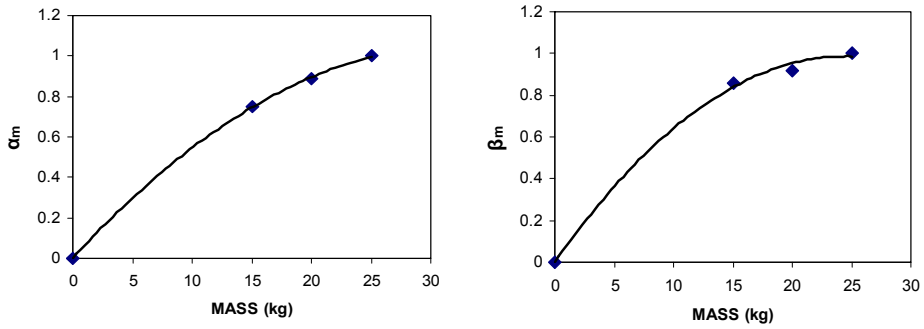

Table 2 Peak damper force and velocities in each mass of pendulum at constant current 1 ampere

Mass of pendulum, m_p (kg)	*Peak force, F_{peak} (N)*	*Peak velocity, v_{peak} (m/s)*
0	0	0
15	4,248	3.85
20	5,045	4.10
25	5,698	4.46

The function of the dimension less parameter, β_m is to measure the velocity of the damper at the different pendulum mass and it is the ratio of the peak velocity of the damper based on the velocity of the damper at mass 25 kg. The equation of the dimension less parameter for velocity damper is shown below:

$$\beta_{m(mass\ of\ 10,\ 15\ and\ 25\ kg)} = \frac{v_{speak\ (mass\ of\ 10,\ 15\ and\ 25\ kg)}}{v_{speak\ (mass\ of\ 25\ kg)}} \tag{5}$$

where

v_{peak} the peak velocity of the damper at each of pendulum mass.

To find the velocity of the damper in the variations mass of the pendulum, the curve fitting is build up between dimension less parameter, β_m and the mass of pendulum for each data that contain in Table 2. The curve fitting is as shown in Figure 4. If the pendulum mass is 25 kg, the dimension less for the velocity, β_m is equal to one.

The equation of the dimension less parameter, β_m after curve fitting is:

$$\beta_m = -0.0016388\left(m_p\right)^2 + 0.0804377 m_p \tag{6}$$

In the experiment, the impact loading is occurred at time 0.001 s. So in the modelling, the time for mass of pendulum start to collide is set as below:

$$\begin{aligned} m_p &= 0 && \text{if} \quad t < 0.001s \text{ (unloading boundary)} \\ m_p &= \text{mass of pendulum} && \text{if} \quad 0.001s < t < t_c \text{ (impact loading boundary)} \\ m_p &= 0 && \text{if} \quad t < t_c \end{aligned}$$

In case to find the time contact, t_c of the pendulum during collision in the variations mass of the pendulum, the linearization is done as shown in Figure 5 between the time contact, t_c and the mass of pendulum for each data in Table 3. The equation of the time contact, t_c after linearization is:

$$t_c = 0.001144 m_p \tag{7}$$

Figure 5 Linearisation of the time contact, t_c depends on the mass of pendulum (see online version for colours)

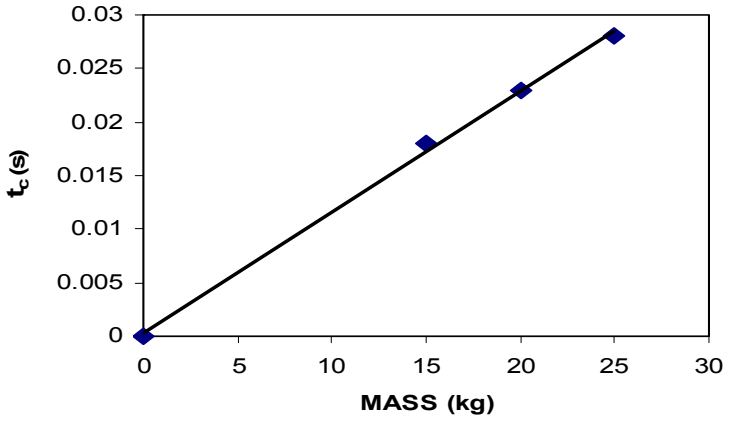

Table 3 Time contact each mass of pendulum

Mass of pendulum, m_p (kg)	*Time contact, t_c (s)*
0	0
15	0.018
20	0.023
25	0.028

In order to build an MR damper model for both simulation and real-time control systems, the proposed modelling approach is developed based on the experimental data and consists of four main. In the first step, experimental works on investigating the force versus time and velocity versus time curve of MR damper behaviour are performed for a set of constant values of applied current namely 0, 0.5, 1, 1.5, 2 ampere and the mass of pendulum is set 25 kg as the impact load for MR damper. The second step is obtaining the hard points for fluid locking region of experimental data from step one as illustrated in Figure 6. In the fluid locking region, the hard point for force and velocity is between times 0.001 to 0.002 s. Then, the third step is fitting the curve by the polynomial function for the hard points in this region. At this region, the velocity of the MR damper is zero. But the force that transmitted of MR damper is fitting by a polynomial function with the first order or □inearization curve of polynomial that shown in Figure 6. The function of the polynomial for the transmitted force and velocity of the damper in the fluid locking region expressed as follow:

$$f_d = \sum_{i=0}^{n} a_i t^i,\ n = 1 \qquad \text{if} \qquad 0.001 \le t \le 0.002 \tag{8}$$

$$v_d = 0 \qquad \text{if} \qquad 0.001 \le t \le 0.002 \tag{9}$$

where f_d is the transmitted force, a_i is the experimental coefficient to be determined from the curve fitting and t is the time during the impact.

Figure 6 Linearisation curve that obtain the hard point in force versus time for fluid locking region (see online version for colours)

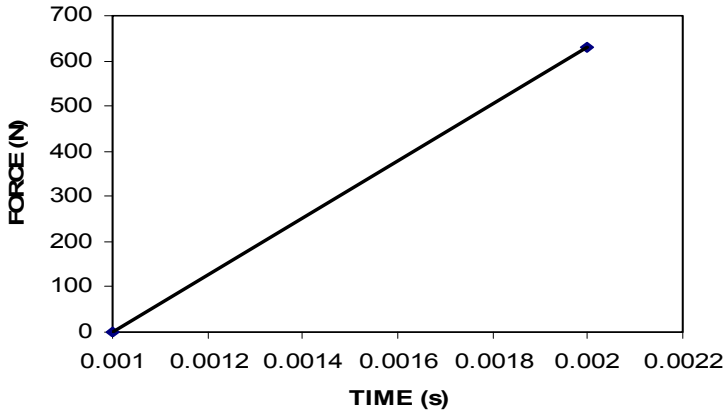

The fourth step is □inearization of the coefficient a_i for each curve. In this step, the coefficient of a_i is linearly approximated with respect to the input current (Choi et al., 2001). The □inearization of the coefficient a_i is governed as follows:

$$a_i = b_i + c_i I \tag{10}$$

After substituting equation (10) into equation (8), the damping force can be expressed as follows:

$$f_d = \sum_{i}^{n} \left(b_i + c_i I\right) t^i,\ n = 1 \quad \text{where} \quad 0.001 \le t \le 0.002 \tag{11}$$

The coefficients of b_i and c_i are obtained from the slope and the intercept of the plots as shown in Figure 7. From the investigation, the coefficients of a_i, b_i and c_i are not responsive to the magnitude of the applied current. The values of b_i and c_i used in this study are listed in Table 4.

Table 4 Coefficients of polynomial model for transmitted force in fluid locking region

Fluid locking			
Parameter	*Value*	*Parameter*	*Value*
b_0	–43.654	c_0	–22.668
b_1	43,564	c_1	22,668

Figure 7 The linear regression of the coefficients a_i correspond to the input current for fluid locking region (see online version for colours)

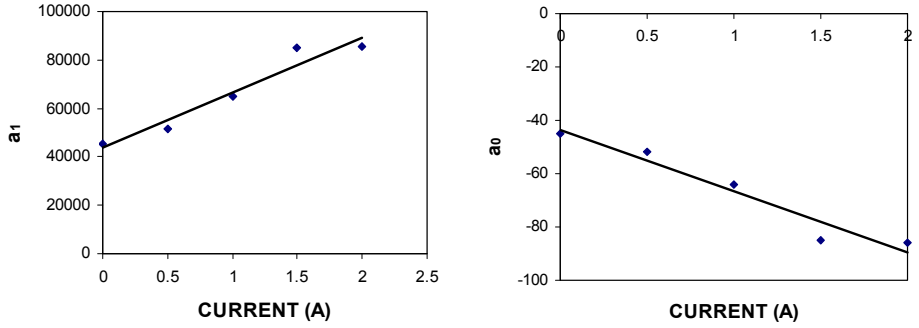

Figure 8 2nd order and 3rd order polynomial curve that obtain the hard point in force and damper velocity versus time for positive acceleration region (see online version for colours)

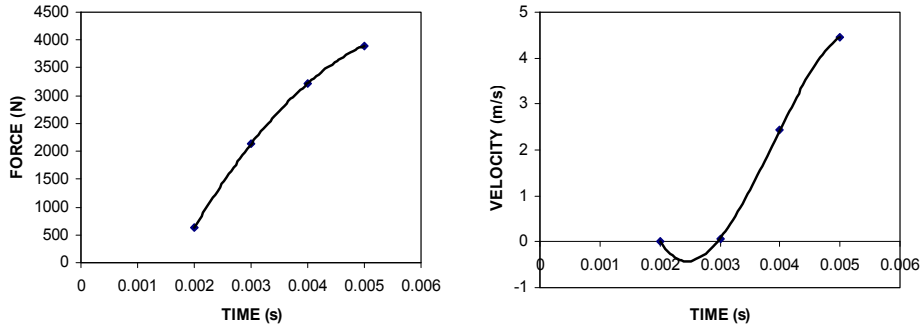

In the positive acceleration region, the proposed modelling approach is developed based on the experimental data and has similar step of modelling with fluid locking region that has been described before. The hard points force versus time and velocity versus time in this region for experimental data is illustrated in Figure 8. It can be clearly stated the hard point in positive acceleration region for force and velocity is between times 0.002 to 0.005 s. This is because from this range of times the velocity of the damper starts to increase and goes to the maximum velocity at time 0.005 s. When the velocity increases, the acceleration of the damper will be positive value and this region is label as positive

acceleration region. At this region, the force that transmitted of MR damper is fitting by a polynomial function with the second order curve of polynomial that shown in Figure 8. The function of transmitted force is expressed as follow:

$$f_d \sum_i^n d_i t^i,\ n = 2 \qquad \text{if} \qquad 0.002 < t \le 0.005 \tag{12}$$

By fitting the hard points in the velocity versus time with polynomial function that shown in Figure 8, the third order of polynomial is chosen to fit it. The function of velocity of the damper is expressed as follow:

$$v_d \sum_i^n g_i t^i,\ n = 3 \qquad \text{if} \qquad 0.002 < t \le 0.005 \tag{13}$$

where f_d is the transmitted force, v_d is velocity of the damper, d_i and g_i are the experimental coefficient to be determined from the curve fitting and t is the time during the impact.

Figure 9 The linear regression of the coefficients d_i in force versus time polynomial curve correspond to the input current for positive acceleration region (see online version for colours)

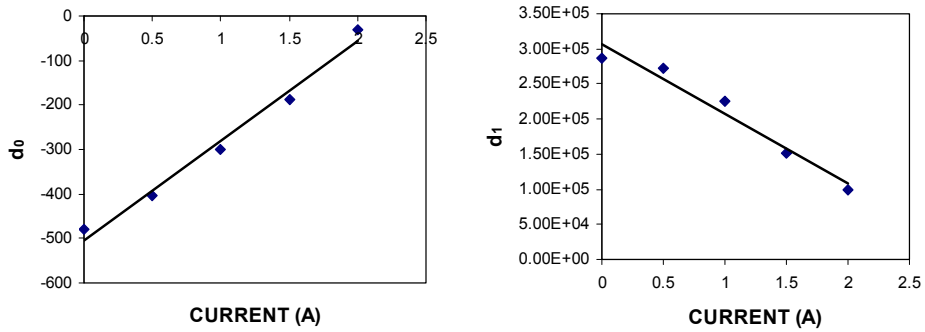

Figure 10 The linear regression of the coefficients g_i in velocity versus time polynomial curve correspond to the input current for positive acceleration region (see online version for colours)

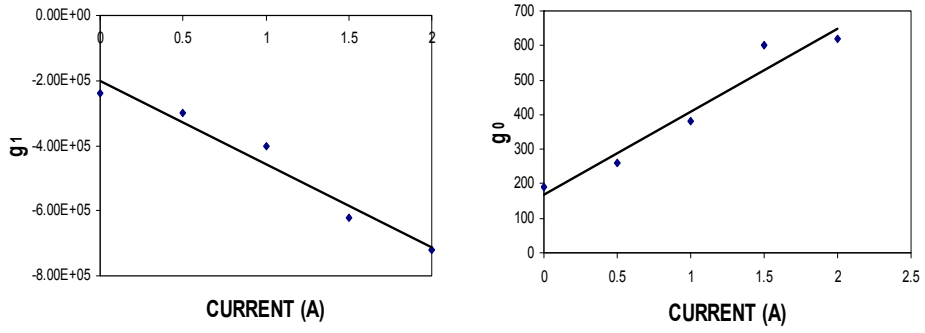

Then the linearization of the coefficients d_i for the transmitted force and g_i for velocity of the damper will be done for each curve. In this step, the both coefficients are linearly approximated with respect to the input current as shown in Figure 9 and Figure 10.

The □inearization of the coefficient for the transmitted force, d_i and velocity of the damper, g_i are governed as follows:

$$d_i = e_i + f_i I, \qquad i = 0, 1, 2 \tag{14}$$

$$g_i = h_i + p_i I, \qquad i = 0, 1, 2, 3 \tag{15}$$

After substituting equation (14) into equation (12), the damping force can be expressed as follows:

$$f_d = \sum_i^n \left(e_i + f_i I\right) t^i, \; n = 2 \qquad \text{if} \qquad 0.002 < t \le 0.005 \tag{16}$$

Then, substituting equation (15) into equation (13), the velocity of the damper is shown below:

$$v_d = \sum_i^n \left(h_i + p_i I\right) t^i, \; n = 3 \qquad \text{if} \qquad 0.002 < t \le 0.005 \tag{17}$$

The coefficients of e_i and f_i are also obtained from the slope and the intercept of the plots as shown in Figure 9 and the coefficients of h_i and p_i also obtained from the slope and the intercept of the plots that described in Figure 10. The values of e_i and f_i used in this study are listed in Table 5 and the values of h_i and p_i are shown in Table 6.

Table 5 Coefficients of the polynomial model for transmitted force in positive acceleration region

Positive acceleration			
Parameter	*Value*	*Parameter*	*Value*
e_0	–499.6864	f_0	146.729
e_1	3.005 × 105	f_1	–9.67 × 104
e_2	–2.749 × 107	f_2	1.359 × 107

Table 6 Coefficients of the polynomial model for velocity damper in positive acceleration region

Positive acceleration			
Parameter	*Value*	*Parameter*	*Value*
h_0	181.776	p_0	243.096
h_1	–2.066 × 105	p_1	–2.342 × 105
h_2	8.464 × 107	p_2	8.874 × 107
h_3	6.182 × 109	p_3	–6.288 × 109

In the negative acceleration region, the proposed modelling approach is developed based on the experimental data. The hard points force versus time and velocity versus time in this region for experimental data is illustrated in Figure 11. Based on the figure, the hard point in negative acceleration region for force and velocity is between times 0.005 to time contact, t_c. In this range of times the velocity of the damper starts to decrease from the maximum velocity at time 0.005 s to zero velocity. If the velocity decreases, the

acceleration of the damper will be negative value and this region is label as negative acceleration region. At this region, the force that transmitted by the MR damper is fitting with the fourth order polynomial curve that shown in Figure 11. The function of the transmitted force is expressed as follow:

$$f_d = \sum_i^n j_i t^i,\ n = 4 \qquad \text{if} \qquad 0.005 < t \le t_c \tag{18}$$

Figure 11 4th order and 3rd order polynomial curve that obtain the hard point in force and velocity damper versus time for negative acceleration region (see online version for colours)

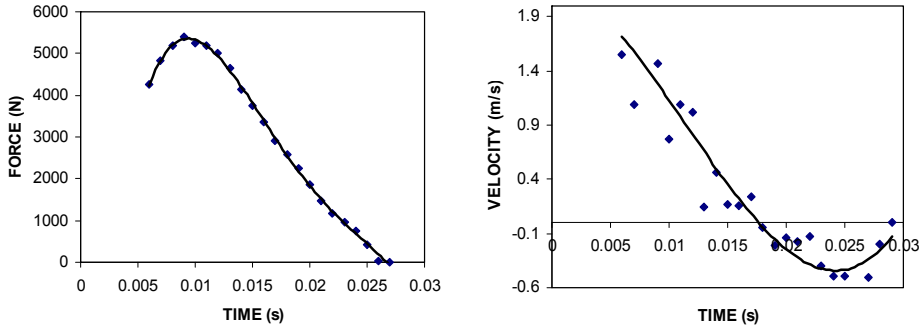

By fitting the hard points in the velocity versus time with polynomial function, the third order of polynomial is chosen to fit it. The function of velocity of the damper is expressed as follow:

$$v_d = \sum_i^n m_i t^i,\ n = 3 \qquad \text{if} \qquad 0.005 < t \le t_c \tag{19}$$

Then the linearization of the coefficients j_i for the transmitted force and m_i for velocity of the damper will be done for each curve. In this step, the both coefficients are linearly approximated with respect to the input current as shown in Figures 12 and 13. The linearization of coefficients is governed as follows:

$$j_i = k_i + q_i I, \qquad i = 0, 1, 2, 3, 4 \tag{20}$$

$$m_i = n_i + r_i I, \qquad i = 0, 1, 2, 3 \tag{21}$$

After substituting equation (20) into equation (18), the damping force can be expressed as follows:

$$f_d = \sum_i^n \left(k_i + q_i I\right),\ n = 4 \qquad \text{if} \qquad 0.005 < t \le t_c \tag{22}$$

Then, substituting equation (21) into equation (19), the velocity of the damper is shown below:

$$v_d = \sum_i^n \left(n_i + r_i I\right),\ n = 3 \qquad \text{if} \qquad 0.005 < t \le t_c \tag{23}$$

The coefficients of k_i and q_i are obtained from the slope and the intercept of the plots as shown in Figure 12 and the coefficients of n_i and r_i also obtained from the slope and the intercept of the plots that described in Figure 13. The values of k_i and q_i used in this study are listed in Table 7 and the values of n_i and r_i are shown in Table 8.

Figure 12 The linear regression of the coefficients j_i in force versus time polynomial curve correspond to the input current for negative acceleration region (see online version for colours)

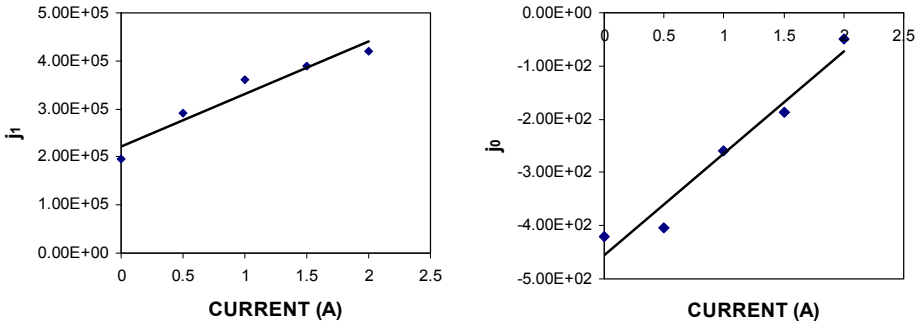

Figure 13 The linear regression of the coefficients m_i in force versus time polynomial curve correspond to the input current for negative acceleration region (see online version for colours)

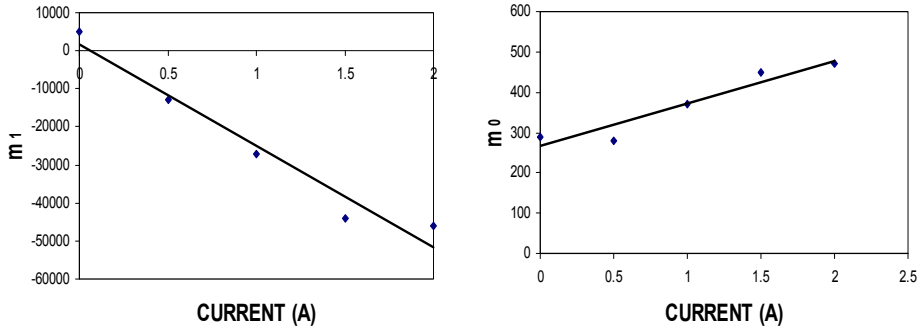

Table 7 Coefficients of the polynomial model for transmitted force in negative acceleration region

Negative acceleration			
Parameter	*Value*	*Parameter*	*Value*
k_0	–453.9306	q_0	–302.6362
k_1	2.291 × 105	q_1	1.113 × 105
k_2	–1.838 × 107	q_2	–1.152 × 107
k_3	5.446 × 108	q_3	4.786 × 108
k_4	–5.375 × 109	q_4	–7.044 × 109

Table 8 Coefficients of the polynomial model for velocity damper in negative acceleration region

Negative acceleration			
Parameter	*Value*	*Parameter*	*Value*
n_0	293.7498	r_0	69.44732
n_1	50.3556	r_1	–1.405 × 104
n_2	–2.877 × 105	r_2	7.564 × 105
n_3	1.41 × 107	r_3	–1.38 × 107

4 Experimental result and model validation

The MR damper testing under impact loading was done by applying the external force that created by the pendulum mass to the MR damper for different values of applied currents to the damper coils. The response of the MR damper due to impact loading with mass of the pendulum 25 kg was investigated for five constant currents of 0, 0.5, 1, 1.5 and 2 ampere, being applied by the current driver of the MR damper. The measured forces in time domain, the force versus displacement and the force versus velocity characteristics are shown in Figure 14 to Figure 16 respectively. It can be seen from Figure 15 and Figure 16 that the magnitudes of the damping force at the piston displacement and velocity are increases proportionally with the increase of the current applied to the damper coils.

Simulation was performed to explore validity and accuracy of the proposed model in MATLAB-Simulink environment. The response of the proposed model is compared with responses of the experimental data of force versus time characteristics as shown in Figure 17. During simulation study, the mass of pendulum are chosen as 25 kg. The overall comparison of force versus displacement and force versus velocity characteristics under various input currents between experimental data and polynomial model responses are shown in Figure 18 and Figure 19 respectively. From these figures, it can be seen that the proposed polynomial model is able to follow the experimental data in fluid locking, positive acceleration and negative acceleration regions.

Figure 14 Measured forces for five constant current levels

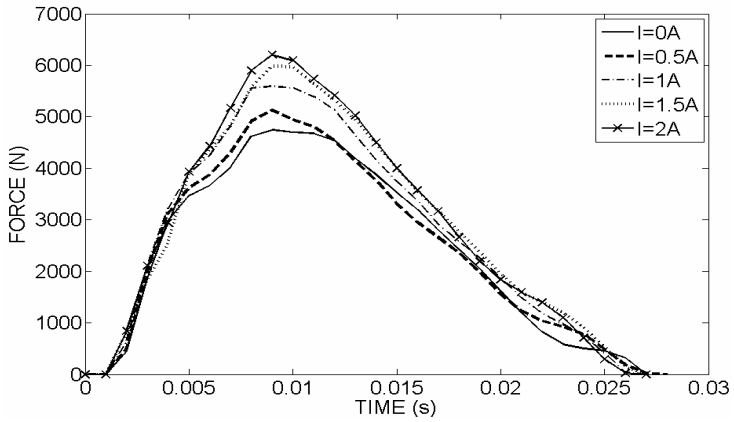

Figure 15 Force versus displacement characteristic for five constant current levels

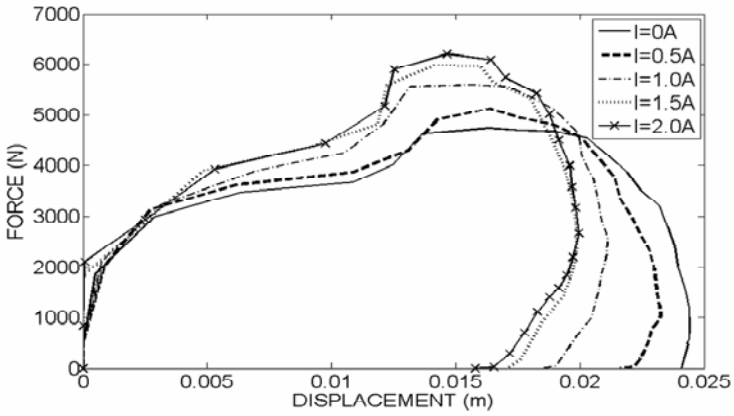

Figure 16 Force versus velocity characteristic for variable current levels, (a) 0.5 ampere (b) 1.0 ampere (c) 1.5 ampere (d) 2.0 ampere

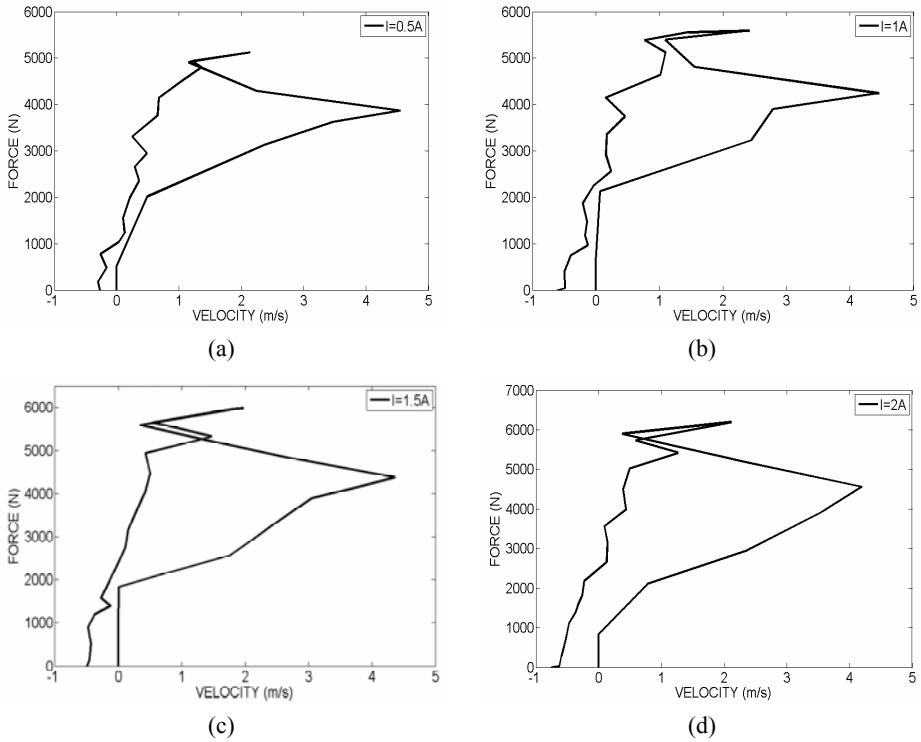

Figure 17 Comparison of the measured and predicted forces versus time for several applied currents, (a) 0.5 ampere (b) 1.0 ampere (c) 1.5 ampere (d) 2.0 ampere

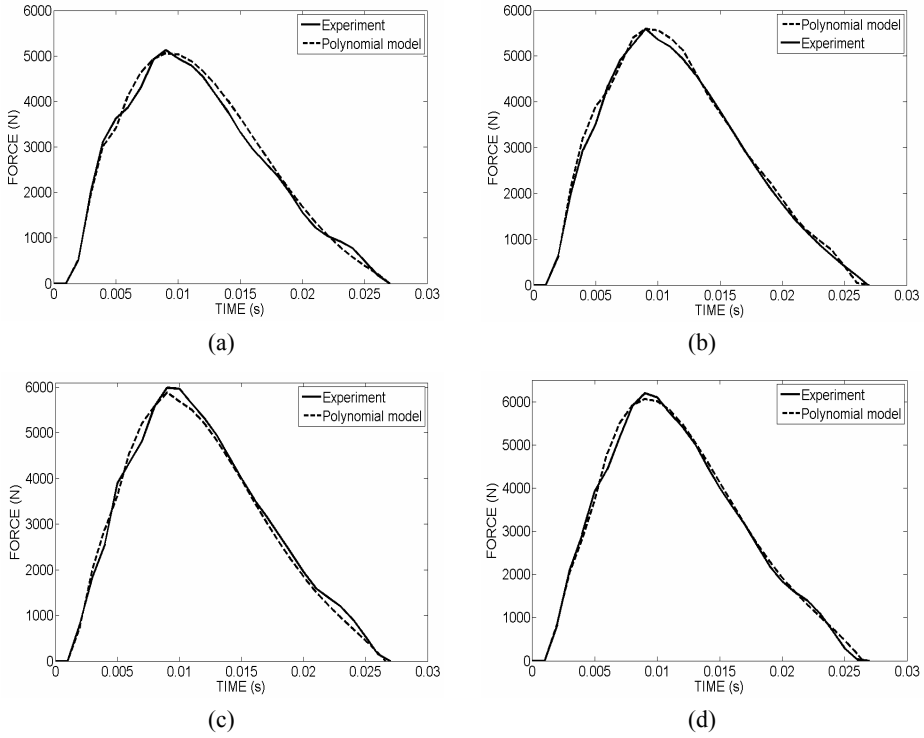

Figure 18 Comparison of the measured and predicted forces versus displacement for several applied currents, (a) 0.5 ampere (b) 1.0 ampere (c) 1.5 ampere (d) 2.0 ampere

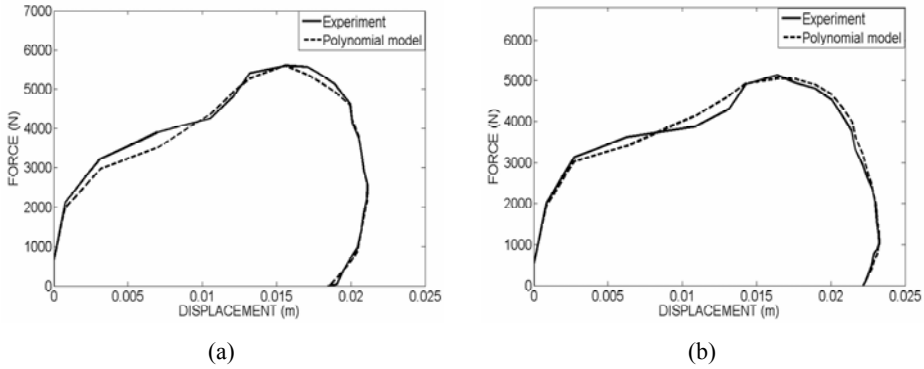

Figure 18 Comparison of the measured and predicted forces versus displacement for several applied currents, (a) 0.5 ampere (b) 1.0 ampere (c) 1.5 ampere (d) 2.0 ampere (continued)

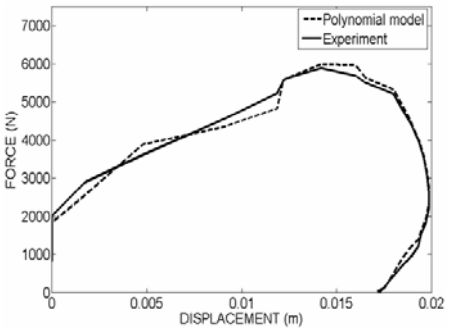

(c)

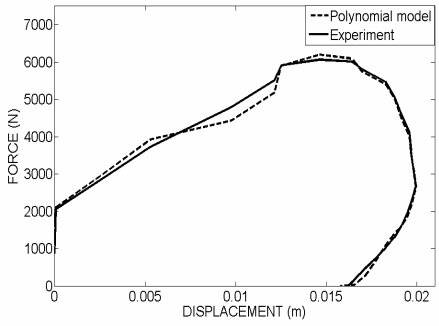

(d)

Figure 19 Comparison of the measured and predicted forces versus velocity for several applied currents, (a) 0.5 ampere (b) 1.0 ampere (c) 1.5 ampere (d) 2.0 ampere

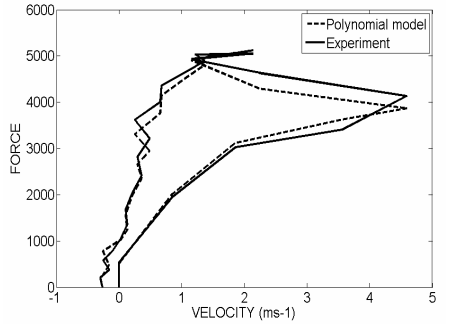

(a)

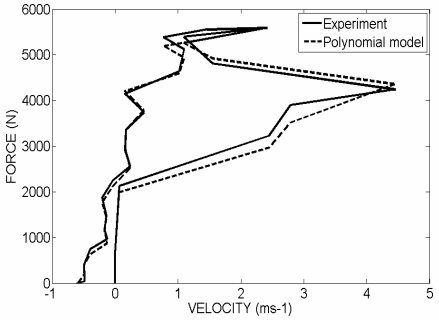

(b)

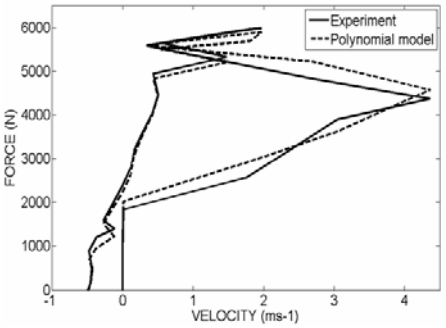

(c)

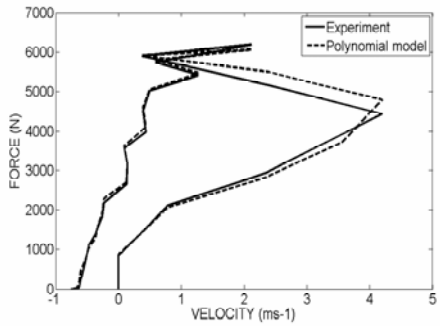

(d)

In order to validate the effectiveness of the proposed polynomial model, the input current will be changed. The measured damping force obtained from experimental work and the predicted force versus velocity from the proposed model are compared as shown in

Figure 20(a) and Figure 20(b), where the pendulum mass and applied current are selected as 25 kg, 0.25 ampere and 1.25 ampere respectively. It is clearly observed that the polynomial model predicts well the force versus velocity behaviour of MR damper at various input currents. Thus, it can be conclude that the polynomial model can predict the damping force at a certain piston velocity under various conditions without re-optimising the coefficients of polynomial model.

Figure 20 Damping force characteristics under various input currents, (a) 0.25 ampere (b) 1.25 ampere

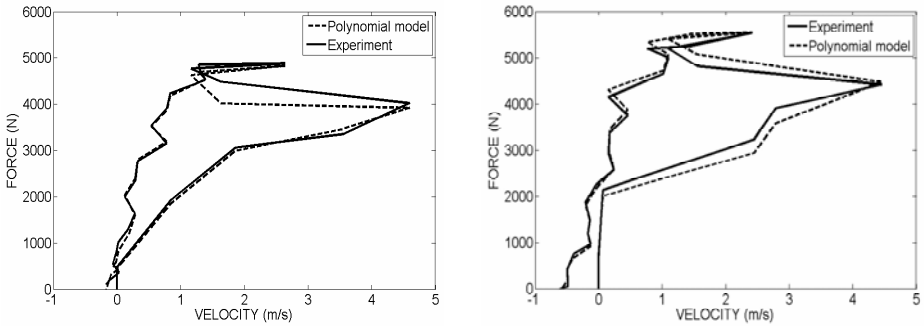

(a) (b)

On the other hands, the characterisation of MR damper under impact loading with three different values of external force by changing the mass of pendulum with 15 and 20 and 25 kg are also been investigated. In this case, the constant current will be applied which is 1.0 ampere. The measured of forces versus displacement and the force versus velocity characteristics are shown in Figure 21 respectively. It can be seen that the magnitude of the damping force at the piston velocity and displacement increases proportionally with the increase of the pendulum mass. This is because the pendulum mass is directly proportional with the force external that applied to the MR damper during impact loading occurred.

Figure 21 Experimental result for (a) force versus displacement and (b) force velocity at variations pendulum mass in constant current applied, 1 ampere

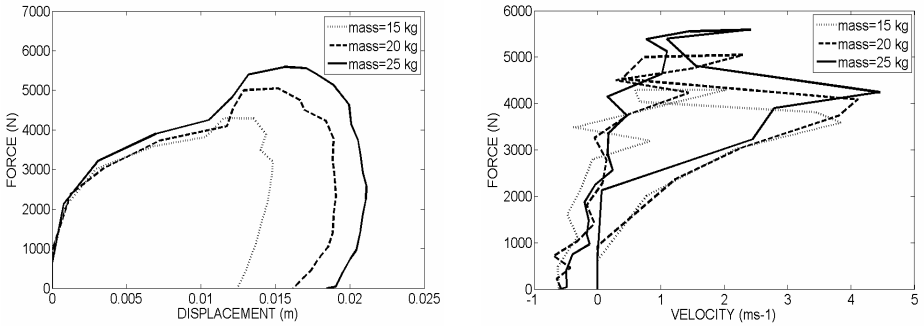

(a) (b)

The hard points of the proposed model are obtained from the experimental data. During simulation study, the applied current and the mass of pendulum are chosen as 1.0 ampere, 15 kg and 20 kg respectively. Figure 22 and Figure 23 show the comparison of force transmitted in displacement and velocity domain under various pendulum mass.

Figure 22 Characteristics comparison for (a) force versus displacement and (b) force velocity at pendulum mass, 15 kg

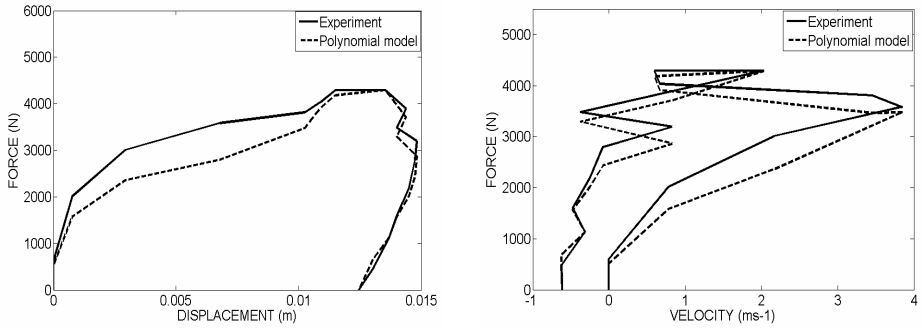

(a) (b)

Figure 23 Characteristics comparison for (a) force versus displacement and (b) force velocity at pendulum mass, 20 kg

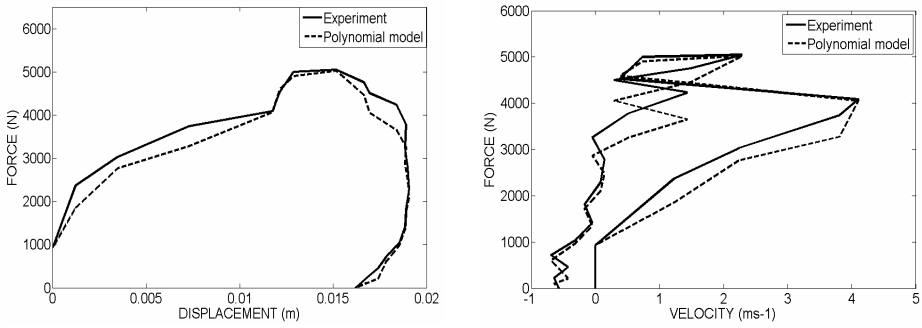

(a) (b)

The overall, the proposed model can obtain the curve in the fluid locking, positive acceleration and negative acceleration region as same as the experiment data. Table 9 is summarises the RMS values and deviation percentages for transmitted force by MR damper under impact loading between the modelling and experiment in variations of current applied and pendulum mass.

As shown in Table 9, the proposed model has the ability to get the data which agreeable with experimental data at various condition of external force (pendulum mass). It is clearly observed that the deviation percentage between experiment and modelling is below 2% which shows that the proposed model is predicts well the transmitted force by MR damper at various input currents. Besides that it can be conclude that the polynomial model can predict the damping force at a certain piston velocity under various conditions without re-optimising the coefficients of polynomial model.

Table 9 RMS values and deviation percentages of the transmitted force by MR damper for modelling and experiment data

Pendulum mass (kg)	*Current (ampere)*	*RMS transmitted force (N)*		*Deviation percentage (%)*
		Modelling	*Experiment*	
15	0	2,464.3	2,501.7	1.49
	0.5	2,538.9	2,505.7	1.32
	1	2,746.1	2,793.9	1.71
	1.5	2,795.7	2.863	2.35
	2	2,977.4	2,981.2	0.12
20	0	2,749.7	2,710.9	1.43
	0.5	2,826.4	2,793.4	1.18
	1	3,106	3,051.5	1.78
	1.5	3,188.3	3,149.1	1.24
	2	3,373.1	3,376.6	0.10
25	0	2,930.4	2,936.8	1.43
	0.5	3,094.4	3,010.1	1.18
	1	3,271.6	3,335.7	1.78
	1.5	3,435.9	3,474.3	1.24
	2	3,592.7	3,561.9	0.10

5 Conclusions

The proposed polynomial model for field-dependent transmitted force of MR damper under impact loading has been investigated in this study. The measured experimental transmitted force was compared with the proposed model. It has been demonstrated that the proposed model has the ability to follow the curve in fluid locking, positive and negative acceleration regions of the MR damper in the form of force versus time, force versus displacement and force versus velocity characteristics. The advantages of the proposed model are in the use of a simple algorithm and do not need a length numerical optimisation for parameter estimation. In future, the proposed model will be connected with the controller system such as inner loop and outer loop controller for semi-active system.

References

Ahmadian, M. and Norris, J.A. (2007) 'Experimental analysis of magnetorheological dampers when subjected to impact and shock loading', *Center for Vehicle Systems and Safety (CVeSS)*, Virginia Tech (MC-0901), Blacksburg, VA 24061, United States.

Ahmadian, M. and Song, X. (1999) 'A non-parametric model for magnetorheological dampers', *Proceedings of the 1999 ASME Design Engineering Technical Conference*, 12–15 September, Las Vegas, Nevada.

Ahmadian, M., Appleton, R. and Norris, J.A. (2002) 'An analytical study of fire out of battery using magnetorheological', *Journal of Shock and Vibration*, Vol. 9, No. 3, pp.29–42.

Ang, W.L., Li, W.H. and Du, H. (2004) 'Experimental and modeling approach of a MR damper performance under harmonic loading', *Journal of the Institution of Engineers*, Vol. 44, No. 4, pp.1–14, Singapore.

Butz, T. and Stryk, O. (1999) *Modelling and Simulation of Rheological Devices*, Tehnische Universitat Munchen, Universitat Augsburg, Preprint, SFB-438-9911.

Chang, C.C. and Roschke, P. (1999) 'Neural network modeling of a magnetorheological damper', *Journal of Intelligent Material Systems and Structures*, Vol. 9, No. 9, pp.755–764.

Choi, S.B., Lee, S.K. and Park, Y.P. (2001) 'A hysteresis model for the field-dependent damping force of a magneto-rheological damper', *Journal of Sound and Vibration*, Vol. 245, No. 2, pp.375–383.

Ehrgott, R.C. and Masri, S.F. (1992) 'Modelling the oscillatory dynamic behaviour of electrorheological materials in shear', *Journal of Smart Materials and Structures*, Vol. 1, pp.275–285.

El Wahed, A.K., Sproston, J.L. and Schleyer, G.K. (2002) 'Electrorheological and magnetorheological fluids in blast resistant design applications', *Mater Des*, Vol. 23, No. 4, pp.391–404.

Giuclea, M., Sireteanu, T., Stancioiu, D. and Stammers, C.W. (2004) 'Modeling of magnetorheological damper dynamic behavior by genetic algorithms based inverse method', *Proc. Romanian Academy*, Vol. 5, No. 1, pp.1–10.

Hengbao, X., Qin, F., Ziming, G. and Hao, W. (2008) *Experimental Investigation into Magnetorheological Damper Subjected to Impact Loads*, Transactions of Tianjin University, Vol. 14.

Hudha, K. (2005) 'Non-parametric modeling and modified hybrid skyhook groundhook control of magnetorheological dampers for automotive suspension system', PhD Theses, Universiti Teknologi Malaysia.

Lee, D.Y., Choi, Y.T. and Wereley, N.M. (2002) 'Performance analysis of ER/MR impact damper systems using Herschel-Bulkley model', *Journal of Intelligent Material Systems and Structures*, Vol. 13, Nos. 7–8, pp.525–531.

McManus, S.J., Steven, S.T., Clair, K.A., Boileau, P.E. and Boutin, J. (2002) 'Evaluation of vibration and shock attenuation performance of a suspension seat with a semi-active magnetorheological fluid damper', *Journal of Sound and Vibration*, Vol. 253, No. 1, pp.313–327.

Peschel, M.J. and Roschke, P.N. (2001) 'Neuro-fuzzy model of a large magnetorheological damper', *Proceedings Texas Section-ASCE*, Spring Meeting, San-Antonio.

Phule, P. (2001) 'Magnetorheological (MR) fluids: principles and applications', *Smart Mater Bull*, No. 2, pp.7–10.

Roschke, P.N. and Atray, V. (2002) 'Neuro-fuzzy control of vertical vibrations in railcar using magnetorheological dampers', Report No. 405450-00112, Association of American Railroads, Pueblo, CO.

Sapinski, B. and Rosol, M. (2007) 'MR damper performance for shock isolation', *Journal of Theoretical and Applied Mechanics*, Vol. 45, No. 1, pp.133–145.

Schurter, K.C. and Roschke, P.N. (2000) 'Fuzzy modeling of a magnetorheological damper using ANFIS', *Proceedings of the 9th IEEE International Conference of Fuzzy System 2000*, 7–10 May, Vol. 1, pp.122–127, San Antonio, Texas.

Sireteanu, T., Ghita, G., Giuclea, M. and Stammers, C. W. (2001) 'Use of genetic algorithms and semi-active fuzzy control to optimize the model and dynamic response of vibration isolation systems with magnetorheological dampers', *Second International ICSC Symposium on Fuzzy Logic and Applications*, Association of American Railroads, Pueblo, CO.

Song, H.J., Choi, S.B., Kim, J.H. and Kim, K.S. (2004) 'Performance evaluation of ER shock damper subjected to impulse excitation', *Journal of Intelligent Material Systems and Structures*, Vol. 13, No. 10, pp.625–628.

Song, X. (1999) 'Design of adaptive vibration control systems with application of magnetorheological dampers', PhD Dissertation, Virginia Polytechnic Institute and State University.

Wang, E.R., Ma, X.Q., Rakheja, S. and Su, C.Y. (2005) 'Force tracking control of vehicle vibration with MR-damper', *Symposium on Intelligent Control*, 27–29 June, Limassol, Cyprus.

Woo, D., Choi, S.B., Choi, Y.T. and Wereley, N.M. (2007) 'Frontal crash mitigation using MR impact damper for controllable bumper', *Journal of Intelligent Material Systems and Structures*, Vol. 18, p.1211.

Yang, G., Carlson, J.D., Sain, M.K. and Spencer, B.F. (2002) 'Large-scale MR fluid dampers: modeling and dynamic performance considerations', *Engineering Structure*, Vol. 24, No. 3 pp.309–323.